DAΦNE TECHNICAL NOTE

INFN - LNF, Accelerator Division

Frascati, May 10, 1995

Note: **MM-6**

THE DAΦNE ACCUMULATOR SEXTUPOLES

B. Bolli, F. Iungo, M. Modena, M. Paris, M. Preger
C. Sanelli, F. Sardone, F. Sgamma, M. Troiani

1. Introduction

The prototype of the Accumulator sextupoles, built by TESLA Engineering (U.K.) has been delivered to LNF on June 21, 1994. The measurement performed on this prototype demonstrated that the magnet meets successfully the requirements of both the DAΦNE Accumulator and Main Rings. Due to the very good results achieved also on the prototype quadrupole built by the same company [1], LNF decided to proceed with the option, foreseen in the contract, of ordering 66 more quadrupoles and 8 more sextupoles to be installed in the Main Rings.

After the prototype acceptance, TESLA Engineering assembled all the Accumulator sextupoles (and quadrupoles).

All other multipoles (11 quadrupoles and 7 sextupoles) were delivered to LNF on April 10, 1995.

The characteristics of the sextupole are recalled in Table 1.

Figure 1 shows a picture of the prototype sextupole with the alignment system on top, while Figure 2 shows the specified pole shape.

The coordinates indicated in this Figure are given in Table 2.

Table 1 - Sextupole parameters

Nominal gradient ($\partial^2B/\partial x^2$, T/m^2)	135
Maximum gradient ($\partial^2B/\partial x^2$, T/m^2)	180
Bore diameter (mm)	108
Pole shape	cubic + straight line
Good field region (mm)	$\pm$ 30
Field quality at magnet center ($\Delta B/B$)	$\leq 5\text{x}10^{-4}$
Magnetic length (mm)	100 $\pm$ 0.3
Amp-turns per pole (A)	3910
Current (A)	280
Turns per pole	14
Copper conductor size (mm^2)	7 x 7
Coolant hole diameter (mm)	4.5
Current density (A/mm^2)	8.5
Magnet resistance (mΩ)	16.9
Magnet inductance (mH)	0.93
Voltage (V)	4.6
Power (kW)	1.38
Water circuits per magnet	1
Total water flow rate (m^3/s)	$2.2\text{x}10^{-5}$
Pressure drop per circuit (atm)	1.5
Water temperature rise (°C)	15
Water initial temperature (°C)	30

Figure 1 - The Accumulator sextupole with its alignment table

Table 2 - Pole Profile coordinates

Point	x(mm)	y(mm)
A	46.76	27.00
B	48.89	23.85
C	51.60	20.85
D	55.12	17.91
E	60.95	13.60
F	65.30	12.46
G	123.20	45.89
H	141.00	15.05
I	141.00	0.000
L	201.00	0.000
M	201.00	31.13
N	164.23	94.82

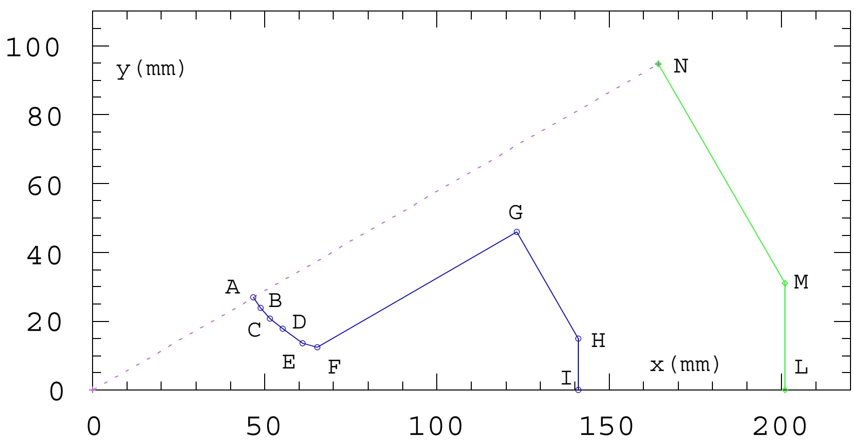

Figure 2 - Sextupole pole profile

2. Electrical Measurements

The resistance of the sextuple prototype has been measured by means of a micro-ohm-meter and by using the Volt-Ampere method. The first measurement is typically a "cold" one, and the measured value is 17.4 mΩ at a room temperature of 21°K.

The second measurement has been performed at the nominal current (280 A). The current was measured by means of a precise DCCT, and the voltage using a standard volt-meter (precision 1÷2 %). The obtained value was 17.14 mΩ.

These results are in good agreement with LNF design value of 17.6 mΩ and the final Tesla one of 16.9 mΩ.

As for other magnets, the resistance and inductance of the sextupole have been also measured at different frequencies by means of the LRC meter HP4284A. The results are shown in Figure 3. The corresponding dc values can be extrapolated from these data. They are in good agreement with the measured data.

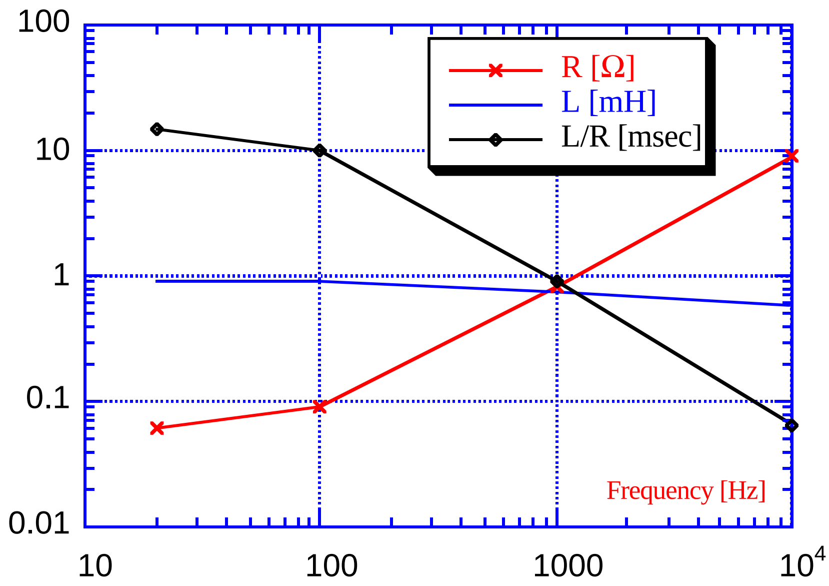

Figure 3 - Resistance, inductance and time constant versus frequency

3. Hydraulic and Thermal Measurements

Hydraulic and thermal measurements have been performed at the nominal excitation current (280 A), with a water flow of 79.2 l/h.

The results are summarized in Table 3.

Table 3 - Thermal and hydraulic measurements on the sextupole prototype

Time [min.]	Iron [°C]	Upper Coil [°C]	Inlet Water [°C]	Outlet Water [°C]
0	22	20.5	20.5	27.5
20	24.5	31.5	20.5	29.5
40	25.5	31.5	21	32
60	26	32	21	32

The pressure drop has not been measured due to the lack of a suitable pressure gauge on the sextupole hydraulic circuit.

4. Magnetic Measurements on the Prototype

The sextupole gradient, defined as the second derivative of the field with respect to the transverse coordinate, is shown in Figure 4 as a function of the excitation current. The behaviour is linear within the specified range. The specified maximum gradient of 180 T/m^2 is reached at ≈275 A. Setting the power supply reference at 280 A, the nominal current for maximum gradient, we measured 281.29 A on the current meter and the corresponding gradient is 183.1 T/m^2, in good agreement with the calculated value.

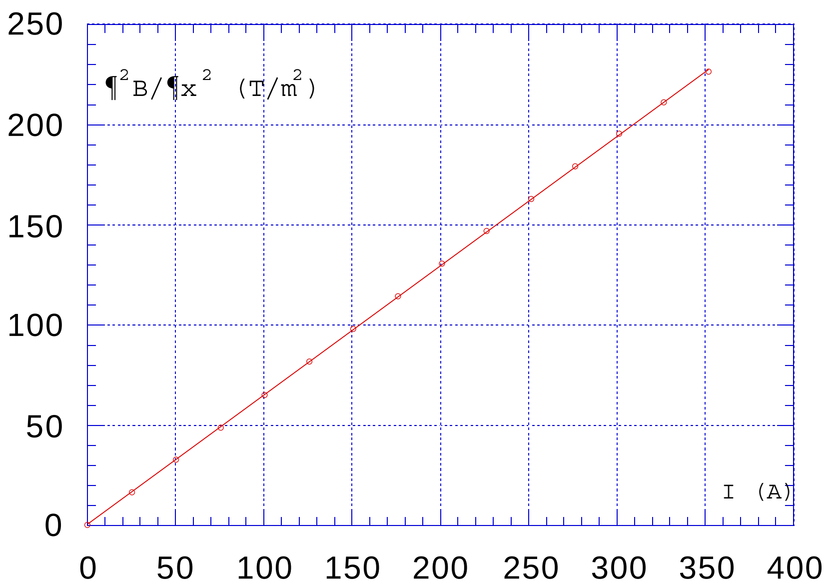

Figure 4 - Sextupole prototype excitation curve

The longitudinal behaviour of the field has been measured by means of a Hall probe driven by a remote controlled 5 axis movement device [2], at different horizontal distances from the magnet axis, the result being shown in Figure 5. Due to the small length to gap ratio, the magnetic length changes by ≈2% in the good field region, and the dependence of the magnetic length on horizontal position is given in Figure 6. The measured length of the magnet exceeds the specified value by ≈ 5%. However, for such a short magnet, the beam dynamics is sensitive only to the integrated sextupole gradient. We decided therefore to accept the magnet without changing the steel length.

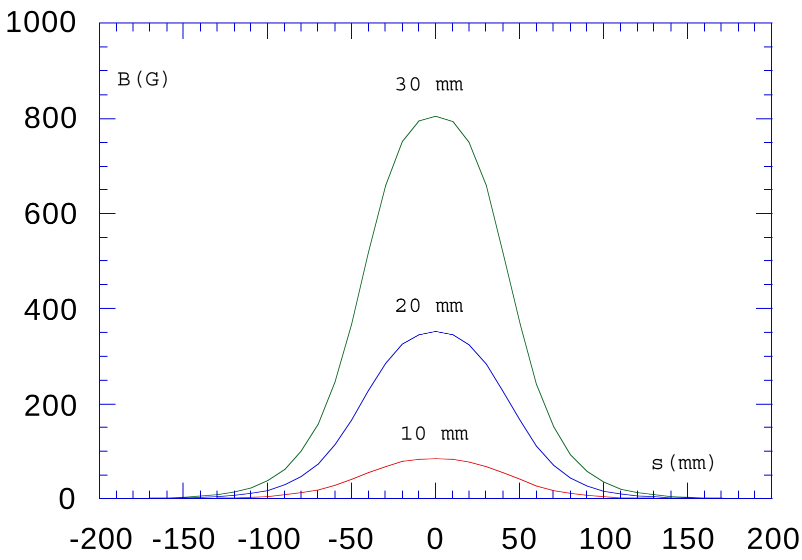

Figure 5 - Longitudinal distribution of the field on the sextupole horizontal symmetry plane at different distances from magnet axis.

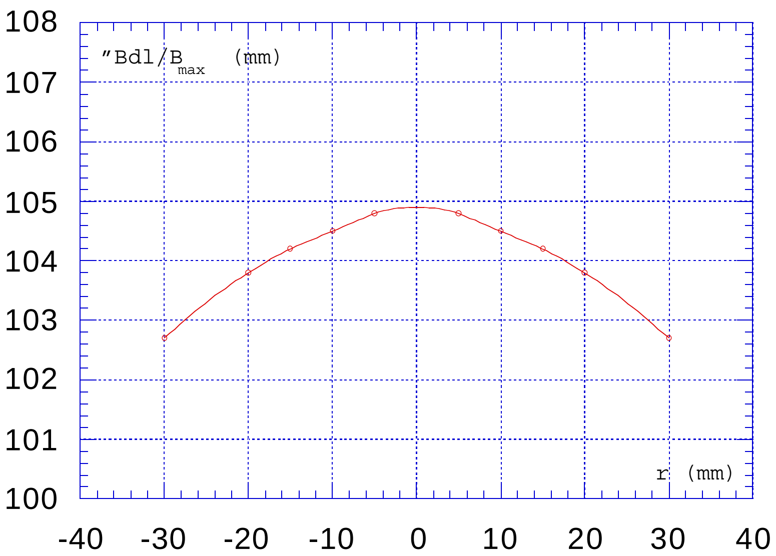

Figure 6 - Magnetic length as a function of distance from magnet axis in the horizontal plane

The specified field quality at the magnet center ($5x10^{-4}$) cannot be checked by means of the Hall probe system, because of to the small value of the field within the good field region and the overall accuracy of the measuring and alignment systems. The specification was set in order to obtain an integrated field quality (including fringe field effects) in the order of 0.1% at the border of the good field region. We measured therefore the integrated field with the rotating coil method [2].

The overall field error is shown in Figure 7 at a distance of 30 mm from the magnet axis, the vector sum of the azimuthal and radial components oscillating between $\approx 0.5x10^{-3}$ and $1.1x10^{-3}$.

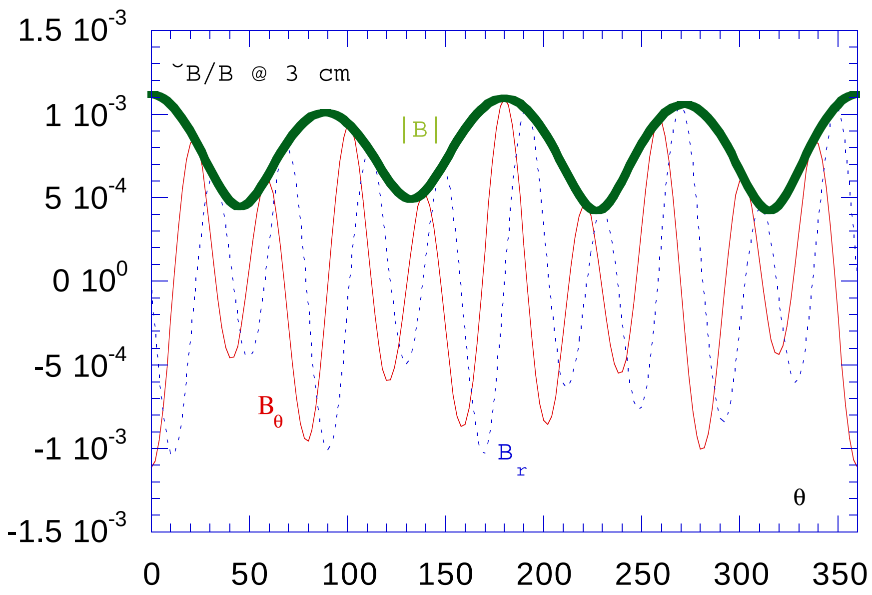

Figure 7 - Fractional contribution of higher order terms to the sextupole field on a circle of 30 mm radius from the axis (thin solid line = azimuthal component, dotted line = radial component, thick solid line = vector sum)

The contributions of higher order terms is given in Table 4. We found, as expected, the largest contribution from the 18-pole ($7.4x10^{-4}$ @ 30 mm from the magnet axis). There is also a non negligible 10-pole field error ($3.1x10^{-4}$), while the other terms are much smaller. It has been checked, by means of tracking simulations, that the obtained result is satisfactory from the beam dynamics point of view.

Table 4 - High order contributions to the sextupole field
@ 30 mm from the magnet axis

Multipole Component	$\Delta B/B$ @ 30 mm
8-pole	6.2×10^{-5}
10-pole	3.1×10^{-4}
12-pole	3.3×10^{-5}
14-pole	3.8×10^{-5}
16-pole	8.4×10^{-6}
18-pole	7.4×10^{-4}
20-pole	3.4×10^{-6}
22-pole	4.8×10^{-6}
24-pole	2.8×10^{-6}

The sextupole has been opened, closed and measured again with no appreciable changes in the high order terms contribution.

5. MAGNETIC MEASUREMENTS ON ALL ACCUMULATOR SEXTUPOLES

As mentioned in the Introduction, seven sextupoles have been delivered at the beginning of April 95, in addition to the prototype, thus providing LNF with all the sextupoles for the DAΦNE Accumulator. At the moment, we are still waiting for the "as built" drawings and Quality Assurance documents.

All the magnets, including the prototype, have been measured with the rotating coil system, in order to check the field quality and the integrated gradient. An accurate alignment system, described in detail in the next paragraph, was available this time. This may account for the discrepancy in the integrated gradient (≈ 0.5%) and in some high order contributions (in particular the 8-pole) between the values measured in July 94 and those measured in April 95 for the prototype (Serial #1).

Figure 8 shows the distribution of the integrated gradient in the eight magnets at a fixed excitation current of 280 A. There is a fluctuation of ≈±0.5% which has to be checked against the QA documents (steel length and bore diameter) for each magnet. In any case, we will ask Oxford Instruments, who is in charge of assembling the magnets on the girders with their vacuum chamber, to group the magnets in such a way that the gradients in each of the two sextupole families are as similar as possible. In this case the first family will be composed of serial # 1,2,3,4, while the second one will contain sextupole # 5,6,7,8.

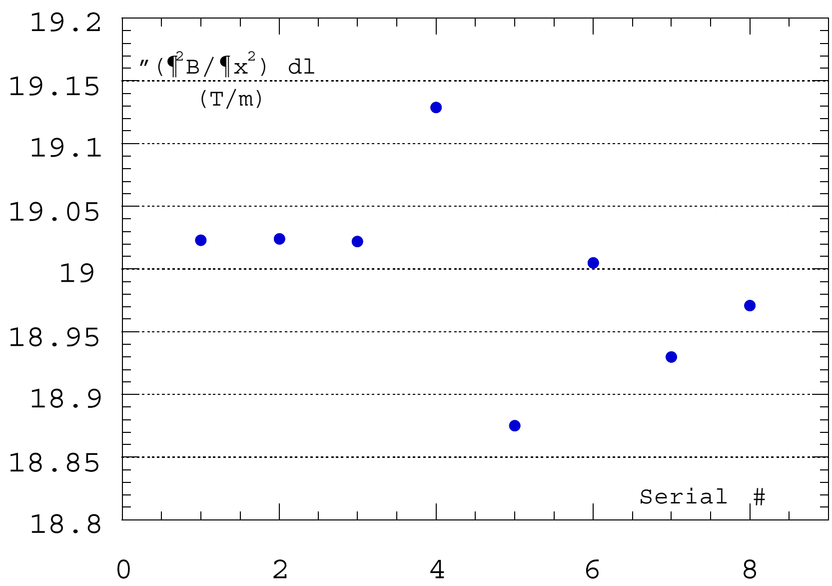

Figure 8 - Integrated gradient of the eight Accumulator sextupoles

The field quality of the magnets is shown in Figure 9. The plot shows the average overall ΔB/B on a circle of 30 mm radius, and the most relevant contributions of high order terms (18-pole, 8-pole and 10-pole). It can be noted that the field quality is remarkably constant over the whole magnet series.

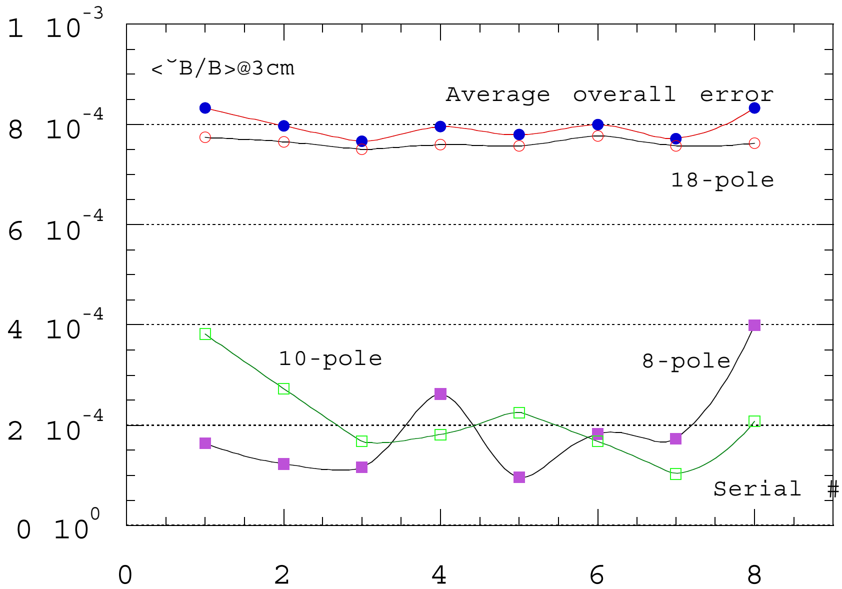

Figure 9 - Field quality @ 30 mm from the magnet axis (full dots = average overall error, empty dots = 18-pole contribution, full squares = 8-pole contribution, empty squares = 10-pole contribution)

6. ALIGNMENT

The rotating coil system yields the horizontal and vertical position of the magnetic center of the sextupoles and the rotation of the symmetry plane with respect to any reference surface where a level can be placed. However, it is insensitive to tilts of the magnetic axis with respect to the coil one. For this reason, we have developed a mechanical prealignment system to minimise this uncertainty [3].

The alignment system (see Figure 1) consists of a precision machined table equipped with two slides driven by micrometric movements in the horizontal plane, while no adjustment is available in the vertical plane. A Taylor-Hobson sphere is mounted on each slide; the distance between the two sphere centers is 99.5 mm. A precision machined cylinder with the same radius as the sextupole bore leans on the three lower poles. An optical target on each side of the cylinder defines the mechanical axis of the magnet. On the upper half of the sextupole there are two machined surfaces parallel to its horizontal symmetry plane. On the first one there are two 20 mm diameter holes near the end faces of the magnet, in the second there is only one of these holes on the magnet center. Three pins are inserted into these holes, each one provided with a horizontal machined surface to match the reference surfaces of the sextupoles. The table leans finally on those three pins.

The slides are moved to align the centers of the Taylor-Hobson spheres on the vertical plane passing through the mechanical axis of the magnet. The height of the spheres is then measured by optical means, thus defining unambiguously the position of the mechanical axis. The absolute accuracy is $\pm 40\mu m$ in the horizontal plane and $\pm$ 20μm in the vertical one. The accuracy on the axis tilt is therefore ± 0.8 mrad and ± 0.4 mrad respectively.

Once measured the position of the mechanical axis, the magnet is automatically aligned by the rotating coil system to find the displacement of the magnetic axis from the mechanical one. We must point out that the system works with a fixed distance of 350 mm between the coil axis and an optical axis defined by a laser beam passing through the sphere centers on top of the magnet. Due to a mistake in the construction of the tables, the distance between the mechanical center of the magnet and the sphere centers is larger by ≈ 0.3mm. However, this distance is measured during the prealignment procedure and we take this effect into account in the evaluation of the vertical distance between the mechanical and magnetic axes. The accuracy of the rotating coil system in the determination of the magnetic center position is $\pm$ 30μm.

We have three such tables, called S1, S2 and S3, for the alignment of the sextupoles.

Table 5 gives the alignment values obtained on the same sextupole (Serial #1) with the three tables. The first row (XAmec) represents the position of the slide holding the first sphere (A) obtained during the mechanical prealignment; the second one (XBmec) is the same for the second one. The third and fourth rows (YAmec and YBmec) give the heights of the two spheres with respect to the mechanical axis.

Table 5 - Alignment parameters of Sextupole #1 with the three tables

	S1	S2	S3
XAmec	12.170	12.030	12.860
XBmec	11.890	11.650	12.080
YAmec (mm)	350.340	350.440	350.360
YBmec (mm)	350.170	350.180	350.250
ΔX (mm)	-0.040	-0.060	-0.070
ΔY (mm)	-0.005	-0.020	-0.020
Φ (mrad)	-0.170	-0.640	-0.660
XAmag	12.210	12.090	12.930
XBmag	11.850	11.580	12.010
YAmag (mm)	350.335	350.420	350.340
YBmag (mm)	350.165	350.160	350.230

The 5-th row (ΔX) gives the distance between the mechanical and magnetic axis. When this value is positive, looking at the magnet on the electrical connection side, the mechanical center is on the right with respect to the magnetic one. This value must be subtracted (with its sign) to XAmec to obtain the position of the slide to define the magnetic axis (XAmag) given in the 8-th row; it must instead be added (with its sign) to XBmec to get the same quantity for the second slide (XBmag) given in the 9-th row.

The 6-th row (ΔY) shows the vertical distance between the mechanical and magnetic axis, after the above mentioned correction. When positive, the mechanical axis is above the magnetic one. This value must be added to both YAmec and YBmec to obtain the heights of the spheres with respect to the magnetic axes. The four last rows contain the indication for the correct alignment of the sextupoles on their girders.

The 7-th row gives the azimuthal tilt of the magnetic horizontal symmetry plane with respect to the mechanical one. When positive, the magnet must be rotated by the same quantity in the counterclockwise direction (always looking at the magnet on the connections side) to avoid the coupling between the two planes.

The horizontal and vertical shifts between the mechanical and magnetic axes should, obviously, not depend on the particular alignment table. The spread in the measured values represents therefore an estimate of the overall alignment procedure.

All the sextupoles have been measured with the first table (S1). The results are given in Table 6.

Figure 10 shows the shifts ΔX and ΔY for the eight magnets. The error bars are obtained by just adding up the overall accuracy of the prealignment system to that of the rotating coil system.

Table 6 - Alignment parameters of the Accumulator sextupoles

	Serial #1	Serial #2	Serial #3	Serial #4	Serial #5	Serial #6	Serial #7	Serial #8
XAmec	12.170	12.010	12.230	12.020	12.110	12.120	12.110	12.100
XBmec	11.890	12.000	11.820	11.920	11.980	12.040	11.940	11.890
YAmec (mm)	350.340	350.280	350.360	350.250	350.340	350.340	350.350	350.300
YBmec (mm)	350.170	350.170	350.260	350.190	350.220	350.170	350.200	350.240
ΔX (mm)	-0.040	-0.070	+0.090	0.000	+0.070	+0.030	+0.040	+0.070
ΔY (mm)	-0.005	+0.015	-0.065	-0.035	-0.050	-0.030	-0.015	-0.045
Φ (mrad)	-0.170	-0.040	-0.440	-0.240	-0.010	+0.340	-0.300	+0.230
XAmag	12.210	12.080	12.140	12.020	12.040	12.090	12.070	12.030
XBmag	11.850	11.930	11.910	11.920	12.050	12.070	11.980	11.960
YAmag (mm)	350.335	350.295	350.295	350.215	350.290	350.310	350.335	350.255
YBmag (mm)	350.165	350.185	350.195	350.155	350.170	350.140	350.185	350.195

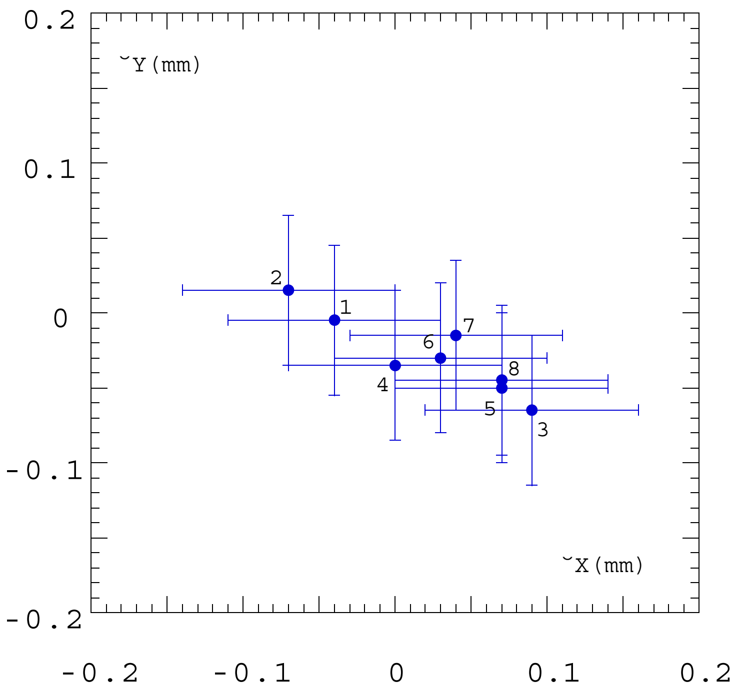

Figure 10 - Distance between mechanical and magnetic centers of the sextupoles

Figure 11 shows the azimuthal rotation of the magnetic horizontal symmetry plane with respect to the mechanical one. Being all measured values well below 1 mrad, we have decided not to correct the magnet positionings by the corresponding amounts.

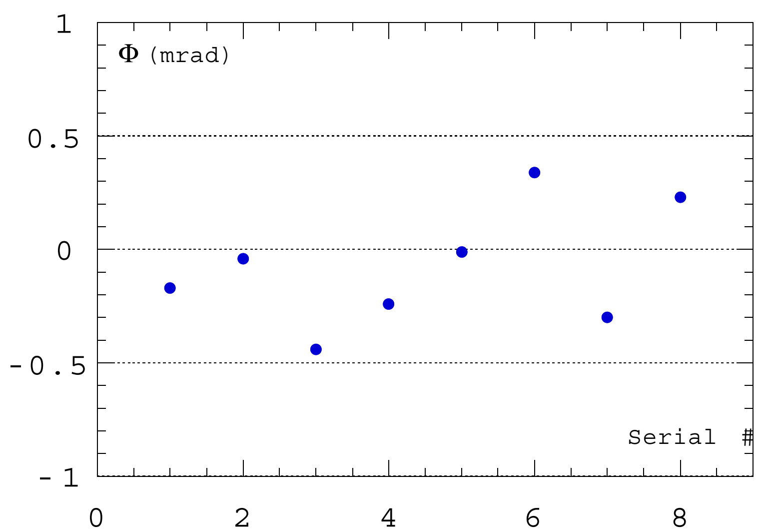

Figure 11 - Azimuthal tilt of the Accumulator sextupoles

REFERENCES

[1] B. Bolli, F. Iungo, M. Modena, M. Preger, C. Sanelli, F. Sgamma, M. Troiani, S. Vescovi, "Measurements on TESLA Quadrupole Prototype for the DAΦNE Accumulator and Main Rings" , DAΦNE Technical Note MM-4 (2/12/94).

[2] F. Iungo, M. Modena, Q. Qiao, C. Sanelli, "DAΦNE Magnetic Measurements Systems", DAΦNE Technical Note MM-1 (4/11/93).

[3] F. Sgamma et. al. , to be published.